This R_1 is over 50 times larger than the largest measured membrane resistance (Table II). This indicates that negligible current flows through the path indicated in Figure A1.

One could lower R_1 by making the lateral current path in Figure 10 smaller. However, this would make r_{ex} approximately equal to r_{Pt} (Figure 10) and thus the "real" measurement area would be the area of the Pt disk.

Appendix B. Calculation of the Fibril Conductivity

The apparatus shown in Figure 1 provides the bulk resistance of the composite membrane, R_m, which is given by

$$1/R_m = 1/R_f + 1/R_p \quad \text{(B1)}$$

where R_f is the parallel sum of the resistances of the conductive polymer fibrils and R_p is the resistance of the intervening template membrane. Resistance measurements on virgin Nuclepore membranes show that $R_p \gg R_f$. Thus, eq 1 becomes

$$1/R_m = 1/R_f = n/R_i \quad \text{(B2)}$$

where n is the number of fibrils in the measurement area and R_i is the resistance of an individual fibril.

The number of fibrils in the measurement area can be obtained from the data in Table I and the known area of the Pt disk electrode. Thus R_i can be calculated from R_m (eq B2). R_i and the area (A) and length (l) of the fibril (Table I) can be used to calculate the fibril conductivity (σ_{fib}):

$$\sigma_{fib} = l/R_i A \quad \text{(B3)}$$

The above analysis assumes that conductive polymer grows only in the pores and not within the bulk polymer. To test this assumption, we attempted to grow polypyrrole within nonporous polycarbonate sheet. No evidence for PPY growth within the nonporous sheet was obtained, and the resistance of these sheets remained essentially infinite.

Clusters of Immiscible Metals. Iron–Lithium Nanoscale Bimetallic Particle Synthesis and Behavior under Thermal and Oxidative Treatments

George N. Glavee, Carl F. Kernizan, Kenneth J. Klabunde,* Christopher M. Sorensen, and George C. Hadjapanayis

Departments of Chemistry and Physics, Kansas State University, Manhattan, Kansas 66506, and Department of Physics and Astronomy, University of Delaware, Newark, Delaware 19716

Received February 12, 1991. Revised Manuscript Received June 10, 1991

Iron and lithium atoms have been trapped in cold, frozen pentane. Upon warming, atom agglomeration took place to form Fe–Li clusters/particles that incorporated some fragments of the organic solvent. At room temperature very small α-Fe crystallites embedded in a matrix of nanocrystalline Li were obtained. Particle sizes averaged 21 nm with α-Fe crystallite regions of about 2.8–3.8 nm. This ultrafine powder (140 m^2/g surface area) was pyrophoric. Upon allowing slow air exposure, particle growth took place and surface area dropped. However, α-Fe crystallites remained. Rapid air exposure caused intense heating to a dull red heat due to oxidation. Surprisingly, α-Fe particles remained as dominant and were encapsulated and protected from further oxidation by a $Li_2O/LiOH/Fe_2O_3$ coating. Heat treatment of the fresh Fe–Li powder caused phase separation of Fe and Li, with α-Fe crystallite growth. Air oxidation again formed a protective outer layer of $Li_2O/LiOH/Fe_2O_3$. By choice of proper temperature and time of heating the α-Fe crystallite sizes could be controlled. However, upon longer term heating at 470 °C, significant amounts of Fe_3C formed due to α-Fe crystallites reacting with carbonaceous fragments from the pentane solvent. Heating to even higher temperature then caused Fe_3C decomposition to larger α-Fe crystallites and carbonaceous species. Characterization methods included Mossbauer, X-ray powder diffraction, surface area measurements, electron microscopy, elemental analyses, X-ray photoelectron spectroscopy, and differential scanning calorimetry. These results demonstrate, for the first time, that normally immiscible metals can be forced to form metastable clusters by using low-temperature, kinetic growth control methods. Also, the isolation of encapsulated, protected α-Fe and Fe_3C nanoscale particles is a significant finding vis-à-vis new magnetic materials.

Introduction

In recent years we have witnessed a revolution in the synthesis of new materials, especially dealing with ultrafine particles (clusters) of metallic, semiconductor, and insulator materials.[1-3] The likelihood of these new materials being technologically important is very great, especially in the fields of catalysis, magnetics, adsorbents, and photovoltaic cells.

We have been interested for some time in the preparation of new bimetallic particles, which sometimes have shown interesting catalytic properties.[4-6] As an extension of this work, we have turned our attention to magnetic materials[7] and herein report some work on a bimetallic combination of iron and lithium.

To force the combination of metal atoms of two normally immiscible metals, such as Fe and Li,[8] our approach is to use atom clustering at low temperature. In this way kinetic

* To whom correspondence should be sent at the Chemistry Department, Kansas State University.

(1) Andres, R. P.; Averback, R. S.; Brown, W. L.; Brus, L. E.; Goddard, W. A.; Kaldor, A.; Louis, S. G.; Moskovits, M.; Peercy, P. S.; Riley, S. J.; Siegel, R. W.; Spaepan, F.; Wang, Y. *J. Mater. Res.* **1989**, 704.

(2) Steigerwald, M.; Alivisotas, A. P.; Gibson, J. M.; Harris, T. D.; Kortan, R.; Mueller, A. J.; Thayer, A. M.; Duncan, T. M.; Douglass, D. C.; Brus, L. E. *J. Am. Chem. Soc.* **1988**, *110*, 3046.

(3) Gesser, H. D.; Goswami, P. C. *Chem. Rev.* **1989**, *89*, 765.

(4) Klabunde, K. J.; Tanaka, Y. *J. Mol. Catal.* **1983**, *21*, 57.

(5) Tan, B. J.; Klabunde, K. J.; Tanaka, T.; Kanai, H. Yoshida, S. *J. Am. Chem. Soc.* **1988**, *110*, 5951.

(6) Tan, B. J.; Klabunde, K. J.; Sherwood, P. M. A. *Chem. Mater.* **1990**, *2*, 186.

(7) Kernizan, C.; Klabunde, K. J.; Sorensen, C. M.; Hadjapanayis, G. C. *Chem. Mater.* **1990**, *2*, 70.

(8) Moffat, W. G. *The Handbook of Binary Phase Diagrams*; Genium Publishing: Schenectady, NY, 1986; Vol. III.

0897-4756/91/2803-0967$02.50/0 © 1991 American Chemical Society

Scheme I

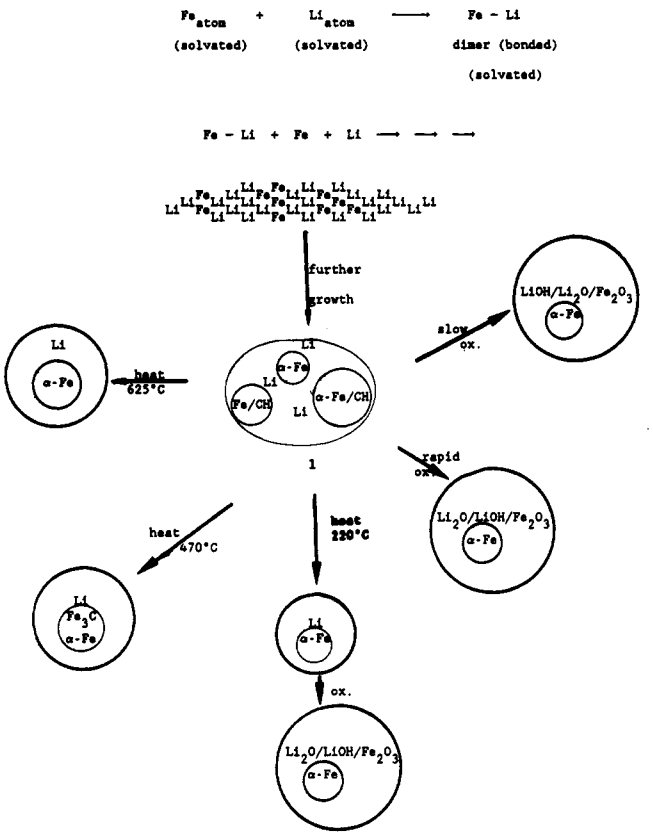

control of cluster growth should prevail.[9] Thus, we have evaporated the two metals simultaneously and trapped the atoms in cold, frozen pentane. When this was warmed, atom migration and subsequent cluster growth took place. The properties and chemistry of the resultant Fe–Li particles are described, and we show how heat/oxidation treatments can yield encapsulated α-Fe crystallites that are protected from the atmosphere by a $Li_2O/LiOH/Fe_2O_3$ coating.

Experimental Methods

General Procedures. Pentane was dried over CaH_2 under N_2. Mossbauer data were obtained at ambient temperature by using a Ranger Scientific Inc. MS-1200 spectrometer, and the X-ray powder diffraction spectra were obtained on a SCINTAG 3000 diffractometer. BET surface area measurements were made on a Micromeritics Flowsorb II 2300 instrument. Heat treatments were carried out under flowing argon in an autoclave equipped with a thermocouple obtained from Parr Instrument Co.

Preparation of Fine Fe-Li Powders in Pentane. The evaporation of the two metals was carried out in a double-electrode metal vapor reactor similar to previously described systems.[10,11] The Fe was vaporized out of an alumina-coated tungsten crucible, and the Li from a ceramic crucible placed in a tungsten basket.

To begin the metal vapor experiment, approximately 20 mL of pentane was first deposited on the walls of the reactor, after which a stepwise warmup of the Fe crucible was initiated. The Fe was heated carefully to the point of evaporation to ensure that no sharp increases in pressure were caused in the reaction chamber. A warmup of the Li crucible was started when a steady evaporation of Fe was evident. The voltage to the Li crucible was increased very slowly since the Li evaporated rather rapidly. Deposition of pentane is continued at a rate of 1–2 mL/min during the evaporation of the metals. Typically, codeposition of Fe (1.22 g, 0.022 mol) and Li (0.365 g, 0.052 mol) vapors were simultaneously codeposited with pentane (200 mL, 1.4 mol) vapor on the walls of a metal atom reactor[10] at 77 K and low pressures (~10^{-3} Torr). After the metals had been evaporated, the Fe–Li/pentane

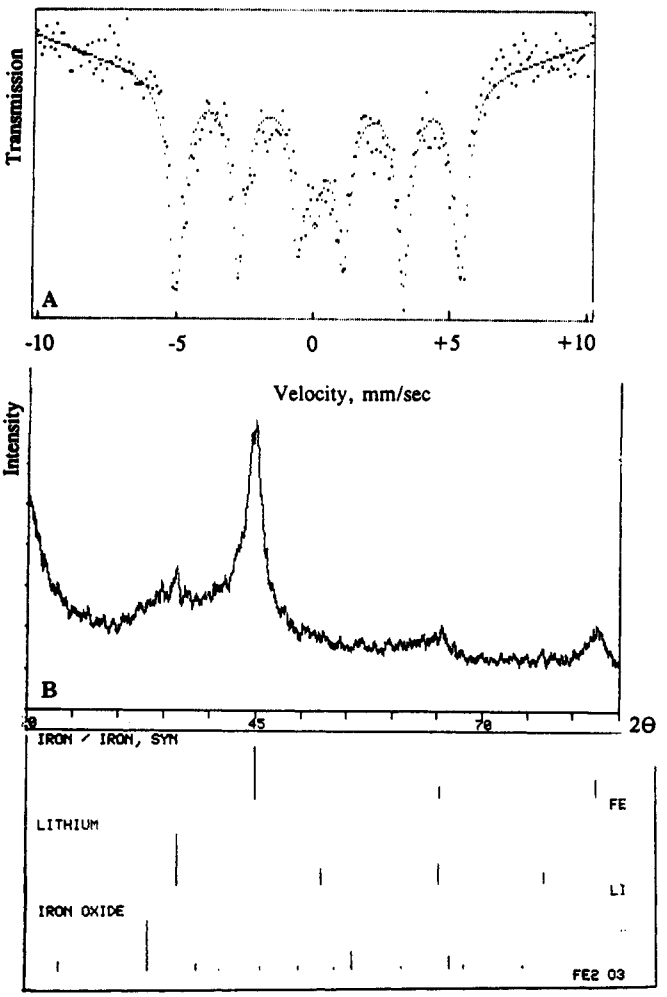

Figure 1. (A) Mossbauer spectrum of Fe–Li (fresh); (B) X-ray powder diffraction spectrum of Fe-Li (fresh).

Table I. Metallic α-Fe Crystallite Sizes (XRD)[a] and Overall Particles Sizes (BET)[b] for Fe–Li Powders Exposed to Oxygen Slowly and Rapidly

sample	XRD crystallite size, nm	BET particle size, nm	surf. area, m^2/g	ratio of BET/XRD sizes
Fe–Li (fresh)	2.8–3.8	21[c]	140	6.4
Fe (without Li, fresh)	2.0	20[d]	118	10
Fe–Li (slow exposure)[e]	8.9	106	12.3	12
Fe–Li (rapid exposure)	18	122	10.6	6.8
Fe–Li (rapid exposure, red heat of oxidation)	29	383	3.4	13
Fe (without Li, rapid exposure, red heat of oxidation)	24	119[e]	9.6	5.0

[a] Using the Scherrer equation $t = 0.9\lambda/B \cos\theta_B$. [b] Using N_2 adsorption and using a measured density of 4.6 g/cm^3. [c] An estimated density of 2.0 g/cm^3 was used in the calculation of Fe–Li (fresh) particle size. [d] An estimated density of 2.5 g/cm^3 was used in the calculation of particle size. [e] A density of 5.2 g/cm^3 was used in calculation of particle size.

(9) Klabunde, K. J.; Jeong, G. H.; Olsen, A. W. In *Selective Hydrocarbon Activation, Principles and Progress*; Davies, J. A., Watson, P. L., Greenbero, A., Liebman, J. F., Eds.; VCH Publishers: New York, 1990; Chapter 13.

(10) Klabunde, K. J.; Timms, P. L.; Skell, P. S.; Ittel, S. *Inorg. Synth.* **1979**, *19*, 59.

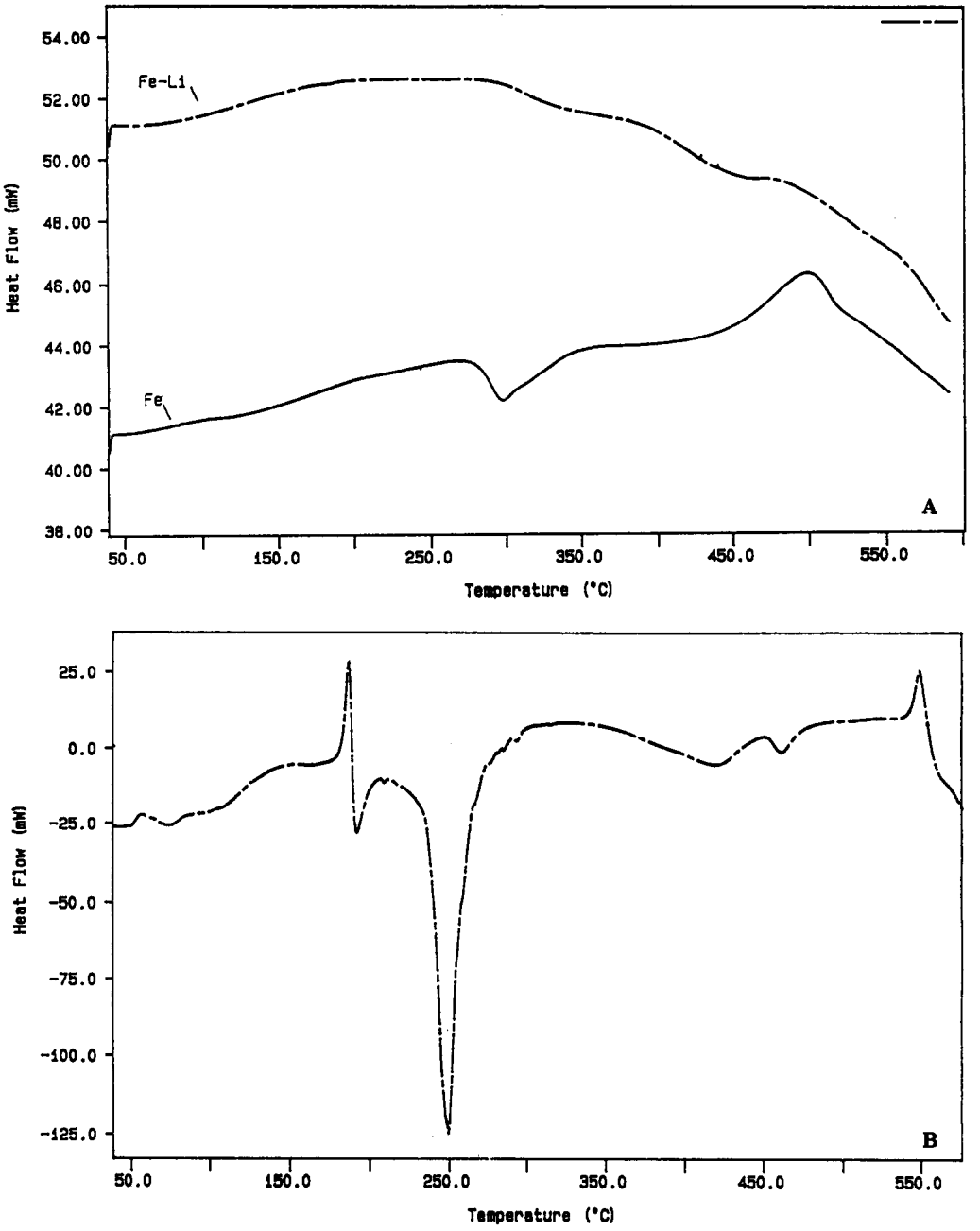

Figure 2. (A) Differential scanning calorimetry of Fe-Li (fresh) and Fe (without Li, fresh). (B) Differential scanning calorimetry of Li powder. The endotherm at 180 °C corresponds to melting, while the strong exotherm at 250 °C probably is due to formation of lithium nitride from the N_2 head gas (an exothermic reaction).

matrix was coated with an additional 50 mL of pentane. The reaction chamber was isolated from the diffusion pump, the dewar containing the liquid N_2 removed, and the matrix allowed to warm (2–3 h) to room temperature. The excess solvent was siphoned off. The remaining product obtained as black, powdery flakes, was dried in vacuo, placed under argon, and transferred into an inert-atmosphere box.

Several metal vapor codepositions were carried out using Fe/Li mole ratios of 2/5 and the amount of product isolated ranged from 1.3 to 1.5 g. Reactions were also carried out using Fe/Li ratios of 1/1, 1/4, and 1/8.

Preparation of Fine Fe (without Li) Particles in Pentane. Iron (1.2 g, 0.02 mol) and pentane (200 mL) were codeposited in a metal atom reactor as described above. Upon workup as described above, 1.0 g of a fine pyrophoric black powder was obtained.

Preparation of Fine Li Particles (without Fe) in Pentane. Lithium (0.35 g, 0.05 mol) and pentane (200 mL) were codeposited in a metal atom reactor as described above. Upon workup as previously described, 300 mg of a greyish pyrophoric powder was isolated.

Oxidation of Fe–Li and Fe (without Li) Samples. Typically ~100 mg of the black powder was placed in a capped vial in the drybox and transferred into a glovebag connected to a cylinder of compressed air. The capped vial was opened slightly to allow diffusion of air into the vial, which was then tightly capped. The sample was agitated by slowly turning the vial around. This process was repeated several times over 1–2 h. The vial was then left slightly opened under an atmosphere of dry air for 6–12 h. For rapid oxidation, the vial containing the black pyrophoric powder was placed in a glovebag. The cap was removed and the vial was slowly turned around as Ar diffused out and dry air diffused in. The temperature of the vial rose significantly.

Heat Treatment of Fe–Li and Fe (without Li) Samples. Approximately 100 mg of the sample was weighed in the inert atmosphere box, capped, and placed in an autoclave equipped with an Ar inlet and outlet and a thermocouple. Argon flow was then initiated and the autoclave placed in a furnace and brought to the desired temperature (usually over 30 min). The autoclave was kept at this temperature over the desired time period and then removed from the furnace and allowed to rapidly cool to or near room temperature under argon (usually between 15 and 30

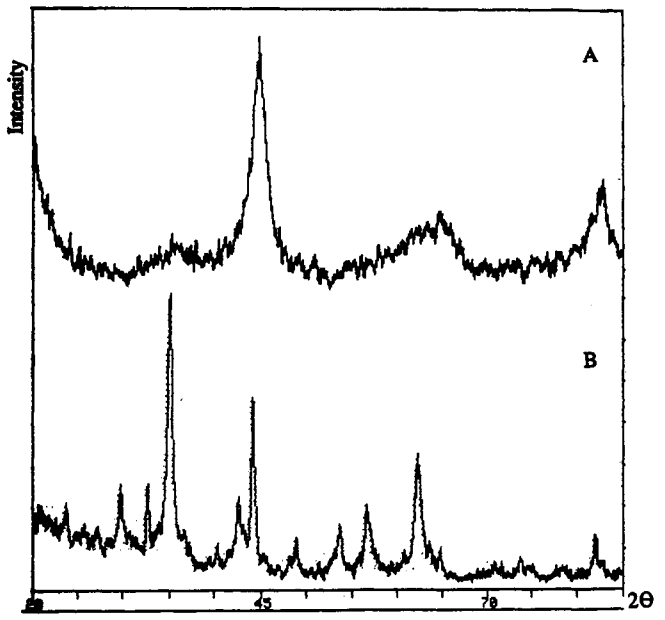

Figure 3. X-ray powder diffraction of (A) Fe (without Li, fresh); (B) Fe (without Li) rapidly oxidized.

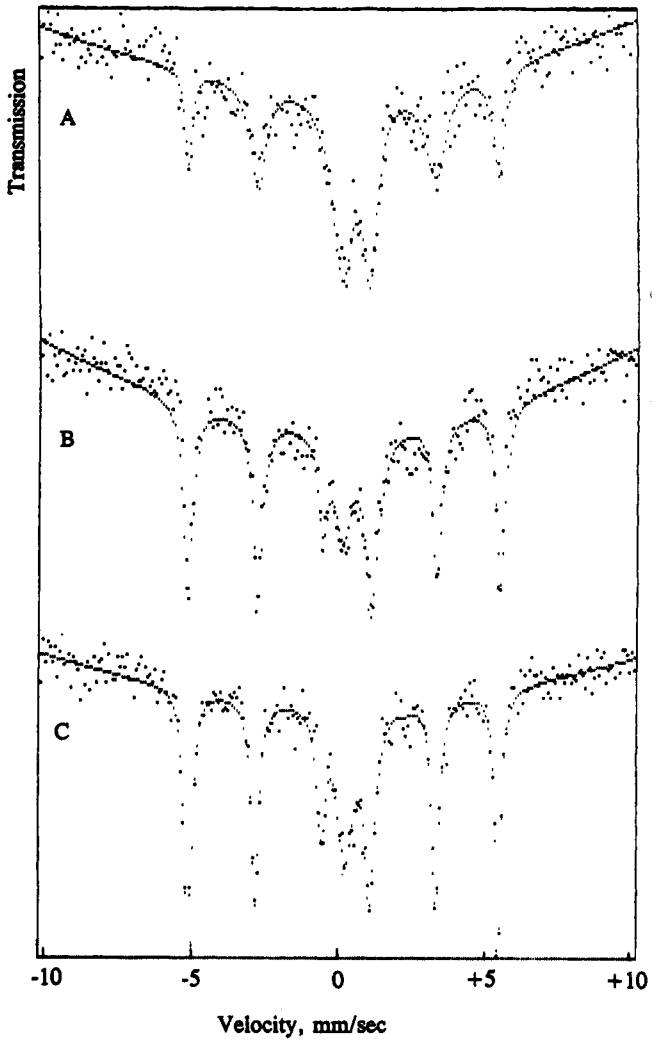

Figure 4. Mossbauer of oxidized Fe-Li samples: (A) slowly oxidized; (B) rapidly oxidized; (C) rapidly oxidized sample that became red hot.

min). The sample vial was quickly transferred and stored in the inert-atmosphere box.

Preparation of Samples for X-ray Powder Diffraction Studies. Fresh Fe–Li and Fe (without Li) samples were coated with mineral oil for protection from oxidation by mixing ~100 mg of the powder and oil to form a paste in the inert-atmosphere box. The paste was then placed in a sample cell, and powder diffraction data were obtained immediately. No such precautions were required for the oxidized and the heat-treated samples. Approximately 100 mg of these air stable powders was placed in the sample cell under ambient conditions, and the powder diffraction data were obtained.

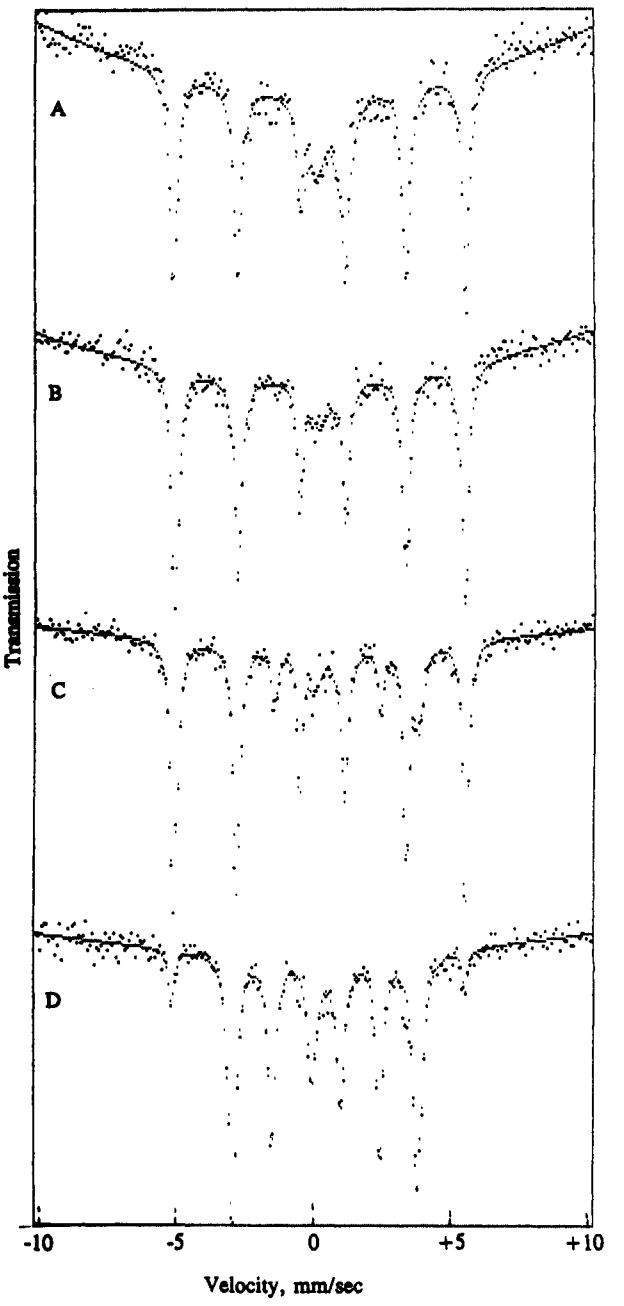

Figure 5. Mossbauer spectra of heat-treated Fe–Li samples: (A) sample heated at 220 °C and oxidized slowly; (B) sample heated at 220 °C and oxidized rapidly; (C) sample heated 470 °C for a short period; (D) sample heated at 470 °C for an extended period.

Preparation of Samples for Mossbauer Spectroscopy. Approximately 50–100 mg of Fe–Li (fresh, untreated) protected with mineral oil as described above was placed in the Mossbauer sample holder made out of aluminum for measurements. The heat-treated and oxidized Fe–Li samples were loaded in the sample cell without protection with mineral oil. Generally, ~300 000 counts were taken for each sample.

Preparation of Samples for Transmission Electron Microscopy. A beaker containing the Fe–Li (~10 mg) sample in 95% ethanol (~5 mL) was placed in a sonicator and agitated for 15–30 min. Three drops of the Fe–Li suspension were then placed

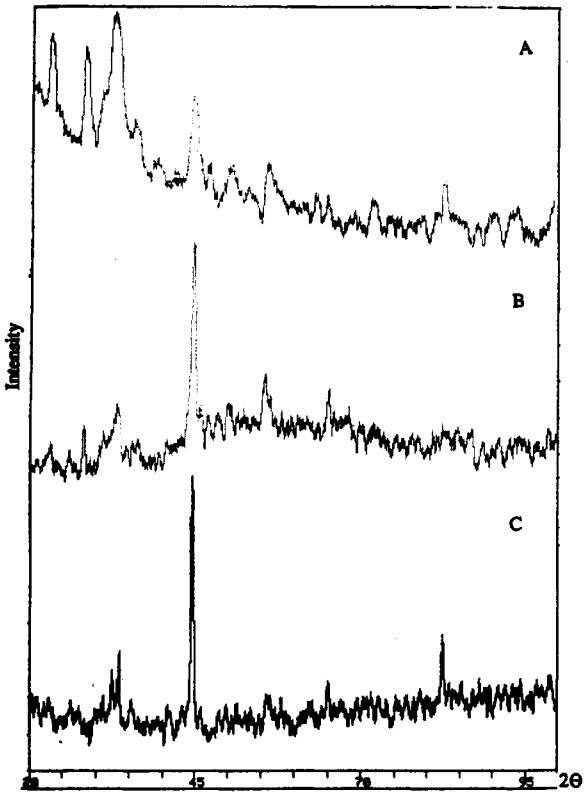

Figure 6. X-ray powder diffraction of oxidized Fe–Li samples: (A) sample oxidized slowly; (B) sample oxidized rapidly; (C) sample that turned to a dull red color during rapid oxidation.

on a carbon-coated grid on filter paper, allowing time for solvent evaporation in between drops.

Preparation of Samples for Differential Scanning Calorimetry. Approximately 6 mg of Fe–Li (fresh, untreated) and Fe (without Li, fresh) powder samples were placed in aluminum vessels and crimped shut in an inert-atmosphere box. The samples were then transferred onto a Perkin-Elmer DSC, and the measurement was done under a flow of N_2.

X-ray Photoelectron Spectroscopy Experiments. X-ray photoelectron spectra of the heat-treated powder were obtained on a Leybold-Heraeus LHS-11 instrument. The X-ray source (Mg Kα, 1253.6 eV) was operated at 60 W, and the vacuum of the sample chamber was 1×10^{-8} Torr. The Fe–Li powder was placed on one side of double-sided Scotch tape under a flow of Ar and inserted into the XPS chamber. Photoelectron lines were recorded for Fe_{2p}, C_{1s}, Li_{1s}, and O_{1s}. Sputtering was carried out using Ar gas for 10–15 min. The C_{1s} (284.6) eV line was used as a reference.

Results and Discussion

It is known that molten iron and lithium do not mix, and so no stable alloy is formed.[8] However, Fe and Li atoms should have at least a weak bonding interaction. Unfortunately we could not locate any literature reports on theoretical treatments of this interaction, although some related work in organometallic chemistry suggests that the interaction would be real and possible.[12] At any rate, we assumed that by allowing the atoms to interact with each other at low temperature, statistics of collisions and kinetic parameters should allow the production of Fe–Li bonded species.

However, as the particle grows an atom at a time, it really cannot be predicted if phase segregtion would occur. For example, if a homogeneous Fe–Li particle were to capture n atoms of Fe and Li, would an iron-rich phase such as metallic α-Fe form and also force the formation

(11) Li, Y. X.; Zhang, Y. F.; Klabunde, K. J. *Langmuir* **1988**, *4*, 385.
(12) Böhm, M. C.; Gleiter, R. *J. Organomet. Chem.* **1982**, *228*, 1.

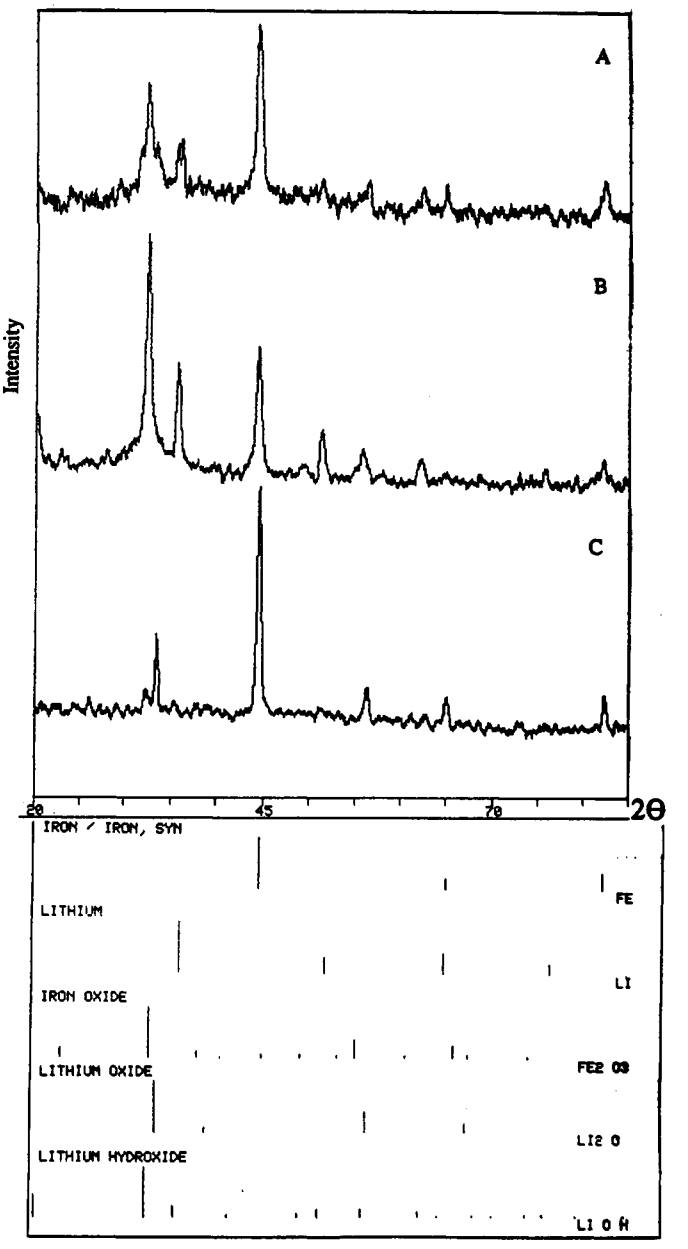

Figure 7. X-ray powder diffraction spectra of heat-treated Fe-Li samples: (A) sample heated to 220 °C and slowly oxidized; (B) sample heated to 220 °C and rapidly oxidized; (C) sample heated to 470 °C prior to oxidation.

of metallic Li phase (Scheme I)? Since we wanted to discourage the formation of the thermodynamically favored metallic α-Fe, we generally used atomic ratios of Li/Fe of 2–8/1, usually 2.5/1, which is shown in Scheme I.

Fresh Samples of Fe–Li. Examination of the fine pyrophoric Fe–Li powder (protected with mineral oil) by X-ray powder diffraction (XRD) and Mossbauer spectroscopy showed broad lines corresponding to metallic α-Fe and Li (Figure 1). Analysis of the XRD data indicated that crystallite sizes were 2.8–3.8 nm for both Fe and Li. Surface area measurements by gas adsorption (BET) methods indicated particle sizes of 21 nm, assuming a spherical shape. The surface area of the fresh Fe–Li powder was about 140 m^2/g (see Table I).

For comparison a sample of Fe particles without Li was prepared in the same way by atom agglomeration in cold pentane. XRD analysis (Figure 2) indicated crystallite sizes of 2.0 nm. BET measurements suggested particle sizes of 20 nm and a surface area of 118 m^2/g (Table I). The XRD analysis of a sample of Li particles similarly

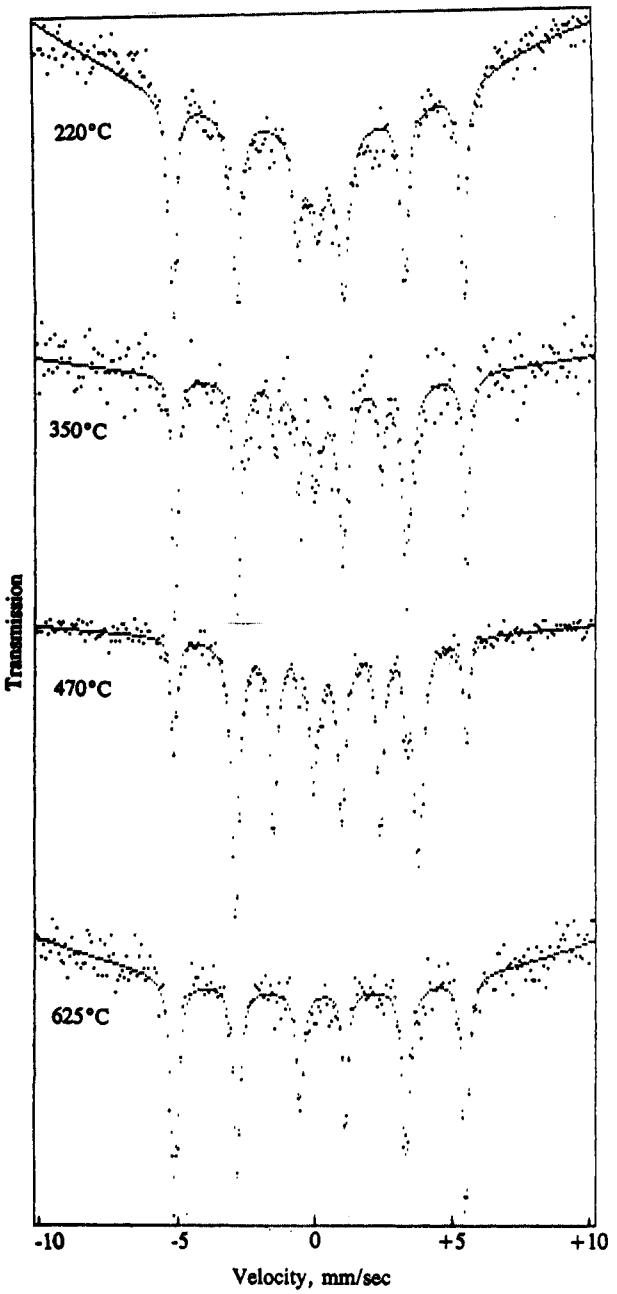

Figure 8. Mossbauer spectra of Fe–Li samples heat treated at different temperatures for 60 min.

prepared yielded crystallite sizes of 17 nm. A surface area of 30 m^2/g was obtained from BET surface area measurement.

The Fe–Li, Fe (without Li), and Li samples were analyzed by using differential scanning calorimetry (Figure 2). Distinct scans were obtained for the three samples, and it is apparent that the Fe–Li powder scan is not a simple superimposition of Li on Fe. In fact, the transitions of the Li sample (Figure 2B) were not observed in the Fe–Li sample. The curves in Figure 2A show an initial endothermic baseline possibly due to the desorption of some of the trapped carbonaceous fragments. There is a distinct exothermic transition at 295 °C for the Fe (without Li) sample. Samples of Fe (without Li) heated at 300 °C for 1 h showed Fe_3C lines in the XRD along with significantly sharper α-Fe lines. Thus the 295 °C exothermic peak could be due to the formation of Fe_3C and the onset of crystallization. Crystallite size of 14.3 nm was obtained for this sample compared with the 2.0 nm obtained for the fresh powder.

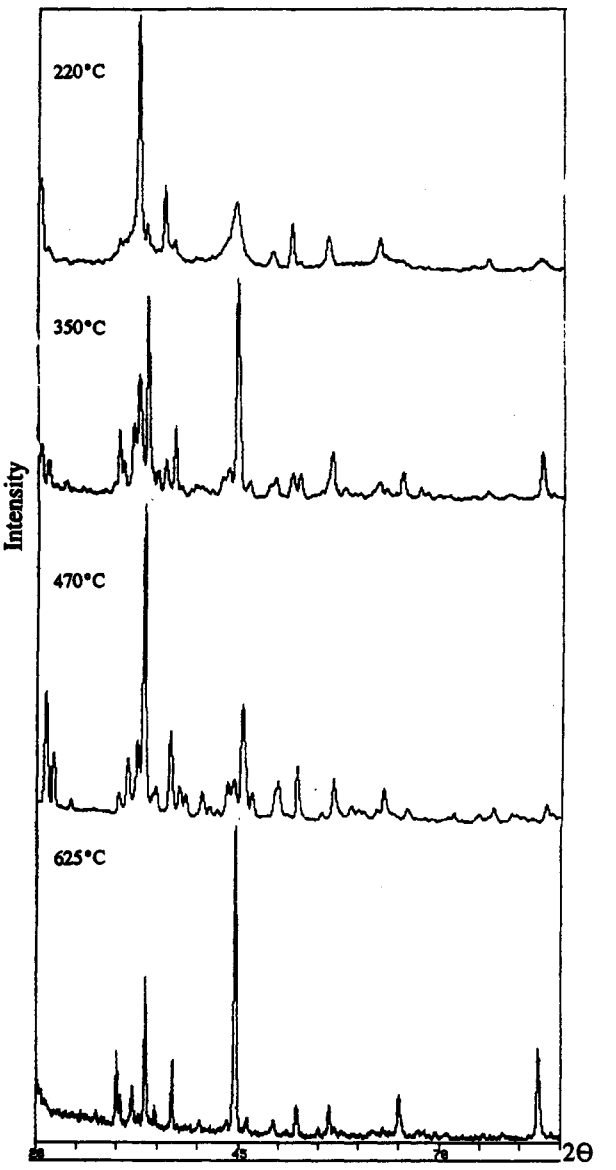

Figure 9. X-ray powder diffraction of Fe–Li samples heat treated at different temperatures for 60 min.

The $\Delta H°_f$ for θ-Fe_3C is 20.9 kJ/mol (endothermic). The fact that we observe an exothermic transition indicates that the small crystallite sizes of the Fe particles and the reactive nature of the carbonaceous groups change the energetics and overcome the expected, small endothermicity (recall that $\Delta H°_f$ corresponds to formation from the pure, crystalline elements iron and graphite). The Fe–Li samples heat treated at this temperature for 1 h also showed the formation of some Fe_3C with α-Fe crystallite size of 12 nm, indicating the inflection in the Fe–Li powder scan at ~325 °C probably corresponds to the onset of iron carbide formation and crystallization.

The endothermic transition observed at 500 °C for the Fe (without Li) scan corresponds to the decomposition of the Fe_3C superimposed on an exothermic position of the curve corresponding to the further crystallization of α-Fe. X-ray powder diffraction of the Fe (without Li) sample heat treated at 500 °C showed only lines corresponding to α-Fe with crystallite size of 42 nm.

Here again our results need explanation. The decomposition of Fe_3C to its elements should be slightly exothermic. However, we observe an endotherm at a temperature corresponding to Fe_3C disappearance and reduction in Fe_2O_3 presence. And since Fe_3C should be

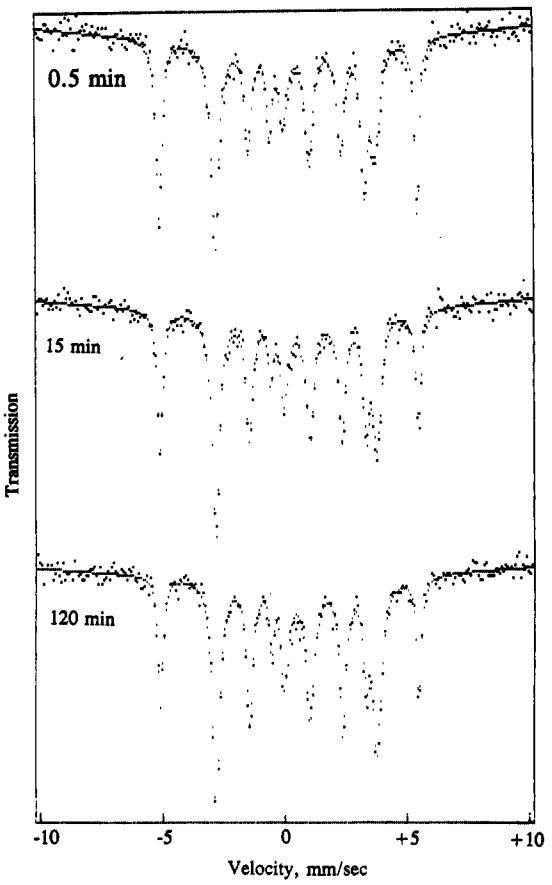

Figure 10. Mossbauer spectra of Fe–Li samples heat treated at 470 °C for varying times.

stable above 500 °C, we believe its disappearance is probably due to at least in part to an endothermic reaction [$3Fe_3C + 2Fe_2O_3 \rightarrow 13Fe(s) + 3CO_2(g)$, $\Delta H°_{rxn} = 366$ kJ/mol]. We note that iron oxides decrease in XRD intensity while Fe crystallites grow during the Fe_3C disappearance. Perhaps this high-temperature chemistry explains the DSC data we obtained.

In considering the Fe–Li DSC and XRD data, the DSC peak at 490 °C on the Fe–Li powder scan corresponds to a similar Fe_3C disappearance. Iron–lithium samples heat treated 500 °C for 1 h showed lines corresponding to α-Fe (crystallite size = 39 nm) and lithium oxide. It is apparent that the presence of the Li does influence the behavior of the powder as evident in the smaller α-Fe crystallite sizes obtained for samples heat treated by using the same conditions and temperatures at which the transitions corresponding to carbide formation and decomposition occur.

Compared with the Fe (without Li) sample, these data suggest that the structure of the Fe–Li particles is best represented by 1 in Scheme I. The broad XRD lines as well as the broad Mossbauer lines require that the α-Fe crystallites be small. However, they are large enough to exhibit long-range order in the Mossbauer (six-line spectrum rather than one line that should be observed for isolated iron atoms or simple paramagnetic iron clusters).[13,14] Therefore, it does not appear likely that any iron *atoms* were isolated in a metallic Li matrix. Rather, during formation some limited phase segregation took place

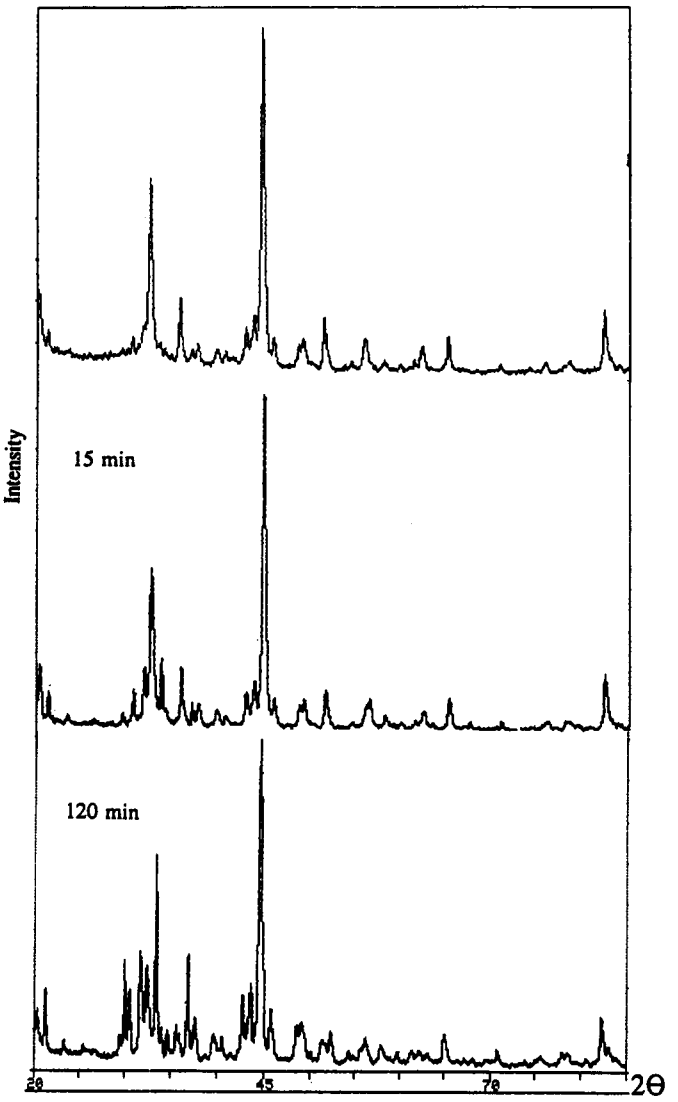

Figure 11. X-ray powder diffraction of Fe-Li sample heated at 470 °C for varying times.

Table II. Metallic α-Fe Crystallite Sizes (XRD)[a] and Overall Particle Sizes (BET)[b] for Fe–Li Powders Treated at Various Temperatures and Various Times

sample	XRD crystallite sizes, nm	TEM particle, sizes, nm	BET particle sizes, nm	surf. area, m^2/g
Fe–Li (220 °C for 1 h)	7.3	29	37	26.2
Fe–Li (350 °C for 1 h)	16	58	61	21.4
Fe–Li (470 °C for 1 h)	26	84	129	8.2
Fe–Li (625 °C for 1 h)	33		424	1.7
Fe–Li (220 °C for 4 h)	14		67	20
Fe–Li (350 °C for 4 h)	19		82	16
Fe–Li (470 °C for 4 h)	32		154	8.4
Fe–Li (470 °C for 2 h)	31	150	154	8.6
Fe–Li (470 °C for 0.25 h)	22	80	138	9.5
Fe-Li (470 °C)[c]	24		132	10.2

[a] Using the Scherrer equation. [b] Using N_2 adsorption and using a measured density of 4.6 g/cm^3. [c] Sample heated to 470 °C as described in the Experimental Section. Cooling to ambient temperature was initiated as soon as autoclave temperature reached 470 °C.

(13) (a) Montano, P. A.; Barrett, P. H.; Shanfield, Z. *Solid State Commun.* **1974**, *15*, 1675. (b) Montano, P. A.; Shenoy, G. K. *Solid* State Commun. **1980**, *35*, 53. (c) Montano, P. A.; Barett, P. H.; Shanfield, Z. *J. Chem. Phys.* **1976**, *64*, 2896.

(14) Nakamura, Y.; Sumiyama, K.; Kataoka, N. *Hyperfine Interact.* **1988**, *41*, 599.

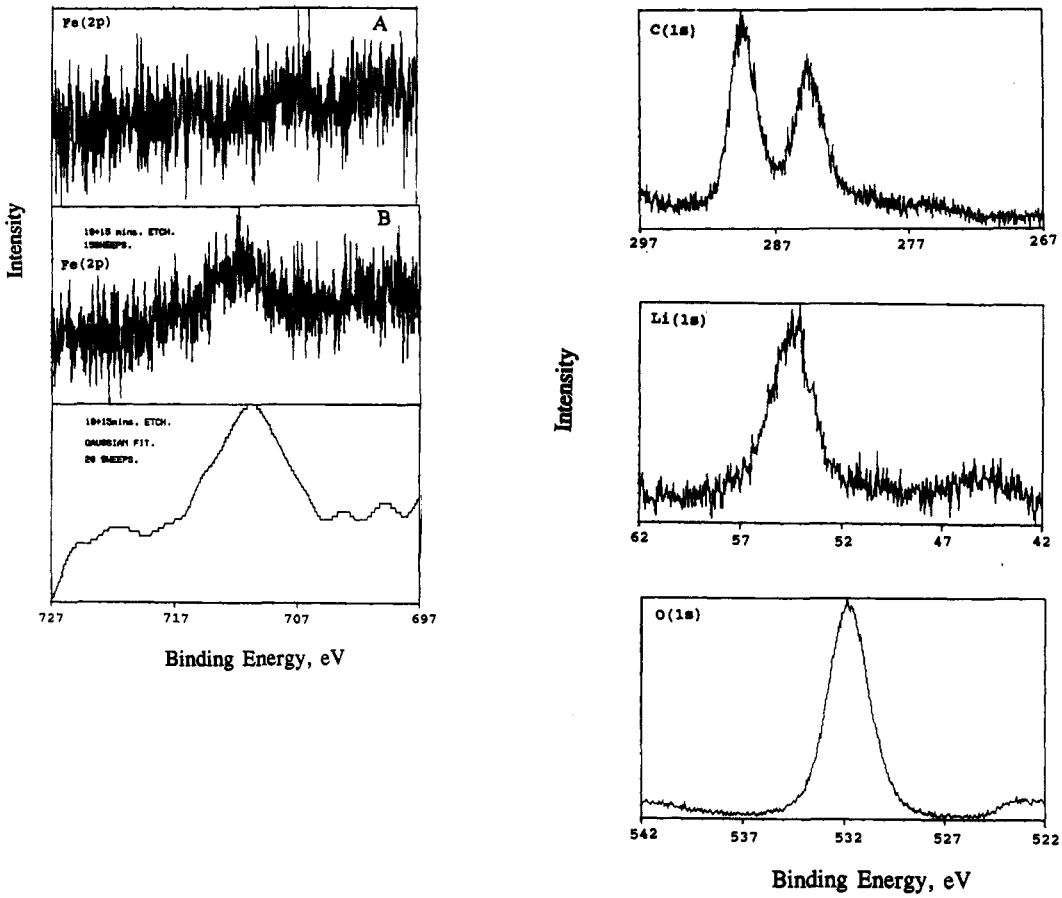

Figure 12. Left: X-ray photoelectron spectroscopy of Fe-Li powder heat treated at 350 °C for 60 min (A) before sputtering and (B) after sputtering. Right: X-ray photoelectron spectra of Fe–Li powder heat treated at 350 °C for 60 min.

leading to a "plum-pudding" structure where very small Fe crystallites are embedded in a larger nanocrystalline Li matrix. The size of the overall particle is that indicated by BET measurements (see Table I).

Thus, we believe that during atom agglomeration in the cold matrix, limited phase segregation occurs. Particle growth to about 20 nm takes place, but each particle is made up of Fe clusters trapped within lithium. Growth is terminated by a complex interplay of surface energy, weak binding interactions between Fe–Li, and continued solvation/fragmentation of pentane as the growth takes place.

We know from previous work that some pentane and fragments of pentane are indeed incorporated into particles of Fe, Co, and Ni,[4,15] and so in structure 1 this is represented by CH_{sol}. Later discussion will show the importance of this carbonaceous material.

Effects of Oxidation. Slow oxidation of the original Fe–Li powder, by inletting small amounts of dry air over 2 h, yielded a material that was mainly made up of metallic α-Fe particles (see XRD (Figure 6) and Mossbauer spectra (Figure 4)). The Mossbauer spectra were punctuated by a doublet with an IS of 0.43 and QS of 0.71, presumably due to small iron oxide particles.[16] The iron oxides were also evident in the XRD along with lines corresponding to Li_2O and LiOH.[17] From the XRD and BET measurements, crystallite sizes for α-Fe were about 8.9 nm, particle sizes of about 106 nm, and surface area of 12.3 m^2/g were found. It is clear that the slow oxidation caused some particle sintering and loss of surface area (compare values in Table I).

These slowly oxidized/passivated samples were stored for 6 months while open to laboratory atmosphere. Even after this time the XRD still showed α-Fe lines along with lines for γ- and α-Fe_2O_3. A conversion of Li_2O and LiOH to $LiOH{\cdot}H_2O$ and subsequently to Li_2CO_3 was also observed over this period.

We found that the rate of oxidation could cause significant changes in the final products. Rapid oxidation of Fe–Li powder yielded a product with very intense XRD lines for α-Fe, crystallite size $\sim$18 nm (Figure 6). The Mossbauer spectra were also dominated by α-Fe lines (Figure 4). Since the rapid oxidation procedure was simply to expose the sample abruptly to air, on some occasions the oxidation caused extreme heating to a dull red color. To our surprise, these products showed even more pronounced XRD and Mossbauer spectra for α-Fe. Crystallite sizes increased to $\sim$29 nm. Gas adsorption studies showed increased particles sizes (380 nm) and much lower powder surface areas (3.4 m^2/g).

The remarkable conclusion based on these data is that rapid oxidation causes heating that leads to Fe–Li phase separation and α-Fe crystallite formation as well as overall particle growth by sintering. Complete oxidation does *not* occur, and in fact the α-Fe particles become encapsulated and protected by an outer layer of $Li_2O/LiOH/Fe_2O_3$. The

(15) Davis, S. C.; Severson, S.; Klabunde, K. J. *J. Am. Chem. Soc.* 1981, *103*, 3024.

(16) Greenwood, N. N.; Gibbs, T. C. *Mossbauer Spectroscopy*; Chapman and Hall: London, 1971, and references therein.

(17) The coexistence of Li_2O and LiOH crystallites was apparent in the XRD. Since the oxidation was carried out under controlled conditions with dry air in a glovebag, the first product is Li_2O. Upon exposure to air, LiOH formed due to H_2O reaction, and then Li_2CO_3 slowly formed due to CO_2 reaction. Thus, at some point during the processing one, two, or all of the components could be detected by XRD.

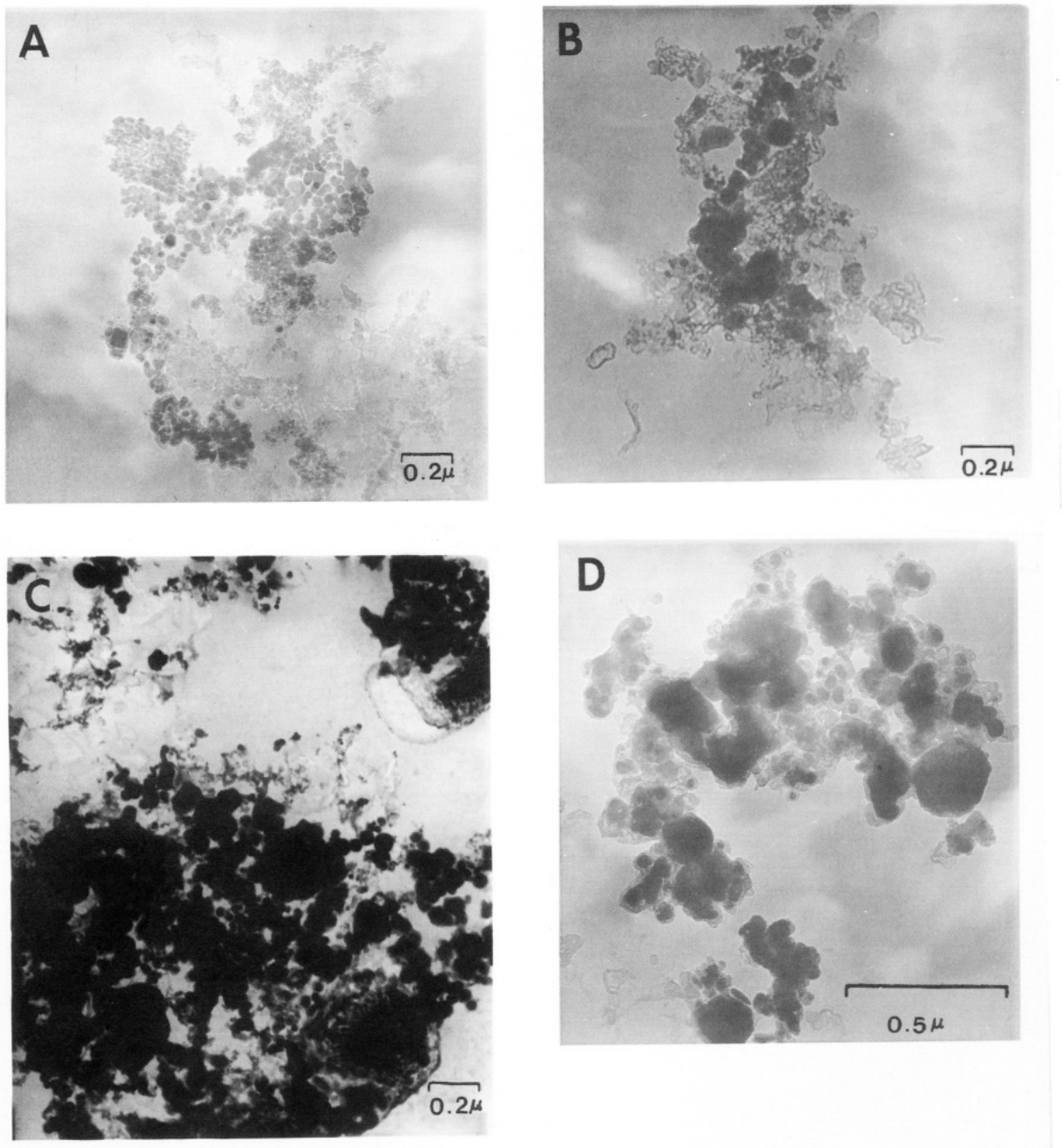

Figure 13. Transmission electron microscopy data of Fe–Li samples: (A) sample heated at 220 °C for 1 h; (B) sample heated at 350 °C for 1 h; (C) sample heated at 470 °C for 1 h; (D) sample heated at 470 °C for 2 h.

protective nature of this coating is impressive. Continued exposure of the rapidly oxidized material to the atmosphere for months did not cause further oxidation. The only change observed by XRD was the growth in crystalline $LiOH{\cdot}H_2O$, which over a 6-month period coverts to Li_2CO_3 apparently due to the effects of atmospheric moisture and CO_2. The α-Fe crystallite size remain unchanged. Scheme I shows in pictorial form what we believe happens.

To compare the protective nature of this lithium-derived coating, the Fe (without Li) sample was also purposely oxidized in the same manner. As expected, XRD confirmed that γ-Fe_2O_3 was the major product, and thus little protection was afforded by a surface iron oxide layer.

Effects of Heat Treatment of Fe–Li Powders. Since the fresh Fe–Li particles are made up of very small crystallites of metallic iron embedded in nanocrystalline lithium and since iron and lithium metals are not miscible at elevated temperatures, it would be expected that heat treatment of 1 would cause further Fe and Li phase separation. We considered that this might be a method of further manipulating α-Fe crystallite sizes, which would still remain coated with Li metal. Subsequent controlled oxidation might yield protected α-Fe particles.

These predictions were indeed borne out under experimental investigation. However, unexpected results were also encountered. Samples of Fe–Li powder were heated under an argon flow to 220 °C and then exposed to oxygen slowly or rapidly. Mossbauer spectra indicated the presence of α-Fe crystallites and the rapidly exposed samples gave sharper lines (Figure 5). Actually, the slowly exposed samples showed more evidence of iron oxide presence (although small), again suggesting that rapid oxygen exposure served to cause growth of α-Fe crystallites followed by rapid "heat encapsulation" (protection by a Li_2O/$LiOH$/Fe_2O_3 coating). XRD analysis confirmed the presence of α-Fe crystallites (Figure 7) along with Li and metal oxide/hydroxide. Crystallite sizes for α-Fe were 12

(slowly exposed) and 18 nm (rapidly exposed), confirming the idea that rapid exposure causes more heating, leading to further α-Fe crystallites growth. Particle sizes by BET were 98 and 146 nm, respectively.

Heating fresh Fe–Li powder to 470 °C for short periods followed by oxygen exposure yielded remarkably clean samples of protected α-Fe crystallites (28 nm, Figures 5 and 7). Subsequent slow exposure or rapid exposure to oxygen did not make a difference in this case. However, heating time caused an unexpected change. When the sample was held at 470 °C for 12 h, the Mossbauer spectra changed dramatically, indicating the formation of Fe_3C[16,18,19] (see figure 5D). This interesting result prompted us to carry out a series of heat treatments for varying times and temperatures. Figures 8–11 show the results. We can see from these studies that heating for 1 h at 220 °C yielded mainly small α-Fe crystallites along with a little iron oxide. Heating at 350 °C for 1 h caused the onset of Fe_3C formation from α-Fe, and 470 °C for 1 h caused a substantial amount of Fe_3C formation. However, heating to the higher temperatures of 625 °C caused only the formation of large α-Fe crystallites, and no Fe_3C was observed. It is possible that Fe_3C was an intermediate, since heating of a 470 °C processed sample (mostly Fe_3C) at 625 °C caused decomposition to α-Fe and Li_2CO_3. The Li_2CO_3 is presumably formed as a result of the reaction of the liberated carbon from Fe_3C with Fe_2O_3 coating, to generate Fe and CO_2, which in turn reacts with Li_2O and LiOH in the coating to generate the carbonate. The conversion of the lithium oxide and lithium hydroxide coating to the carbonate occurs normally under atmospheric condition in samples left on a laboratory bench top over extended periods (3–6 months). XRD spectra confirmed these observations as well as showed contributions for Li_2O/LiOH and small amounts of Fe_2O_3.

A series of experiments at 470 °C with varying times (Figures 10 and 11) showed the evolution of Fe_3C. Table II summarized crystallite and particle sizes as well as surface areas. As expected, higher temperatures yielded larger crystallites and particles and lower surface areas.

There seems to be little doubt that Fe_3C can be formed under the right temperature conditions and can be decomposed to its elements upon heating still hotter (625 °C). Of course we must have a source of carbon for this process to occur. Earlier work has shown that cluster growth in cold pentane causes the incorporation of carbonaceous material (fragments of pentane). It is this carbon, designated as CH in Scheme I, that must be the source of carbon. Elemental analyses of the fresh Fe–Li powders confirmed that 3.81% C and 0.86% H were present. This amount of carbon probably is the limiting reagent in Fe_3C formation since we know that addition of organic polymers such as poly(acrylonitrile) can cause even higher metal carbide yields.[20]

Finally, we should discuss further the aspect of protection of these ultrafine powders from oxidation. We now know how to control α-Fe crystallites sizes by proper choice of heat-treatment temperatures. Formation of Fe_3C can be controlled somewhat, and Scheme I summarizes these findings in pictorial form. The schematic picture is supported by X-ray photoelectron spectroscopy data obtained on Fe-Li powder heated to 350 °C for 1 h. (Figure 12), which showed, Li, C, and O but no Fe on the surface. Upon sputtering, Fe is observed in addition to the other elements. The final powder materials have very small α-Fe crystallite sizes and yet do not change upon exposure to the atmosphere for months at a time. They are indeed well protected by encapsulation by the formed Li_2O/LiOH/Fe_3O_3 coating as evident in the TEM photographs and the BET particle sizes. Furthermore, exposure to the atmosphere over long periods leads to Li_2CO_3 formation, which may be an even more robust protecting coat. These are significant findings. Controlling crystallite sizes of nanoscale materials and protecting them could be of value in the field of magnetic materials. We plan to carry out detailed studies of their magnetic properties and will report on this at a later time.

Acknowledgment. The support of the National Science Foundation through their Materials Chemistry Initiative is acknowledged with gratitude. We are indebted to Dr. John Schlup and Mr. Larry Sieb for the DSC data. We also thank Dr. Yong-Xi Li for the XPS data and for many useful discussions.

Registry No. Fe, 7439-89-6; Li, 7439-93-2; Li_2O, 12057-24-8; LiOH, 1310-65-2; Fe_2O_3, 1309-37-1; Fe_3C, 12011-67-5; pentane, 109-66-0.

(18) Stevens, J. G.; Stevens, V. E. *Mossbauer Effect Data Index*; covering 1966-1968 Literature; 1F1/Plenum: New York, 1975.

(19) Sextets were observed in the room temperature Mossbauer for the α-Fe and Fe_3C particles. This is a result of magnetic splitting and indicates that the crystallites are in the multidomain size range. The sextet for α-Fe shows a hyperfine field of 332 kOe compared to that observed for bulk α-Fe of 330.3 kOe. A hyperfine field of 207 kOe was found for the iron carbide particles, which compares with 208 kOe reported for α-Fe_3C (Maelse, J. A.; Butt, J. B.; Schwartz, L. H. *J. Phys. Chem.* 1978, *82*, 558). Our XRD evidence also suggests Fe_3C. A low-temperature Mossbauer study might be useful in clarifying the spectral region around zero velocity. We intend to carry out a series of such studies and results will be reported in a future report on the magnetic properties of these new materials.

(20) Hooker, P.; Tan, B. J.; Klabunde, K. J.; Suib, S.; *Chem. Mater.* 1991, *3*, 947.